Polystyrene Microplastics Reduce Abundance Of Developing B Cells In Rainbow Trout (*Oncorhynchus Mykiss*) Primary Cultures.

Patty Zwollo[1¶], Fatima Quddos[1], Carey Bagdassarian[2], Meredith Evans Seeley[3], Robert C. Hale[3], and Lauren Abderhalden[1]

[1]Department of Biology, William and Mary, Williamsburg, VA 23185.

[2]Interdisciplinary Studies, William and Mary, Williamsburg, VA 23185

[3]Virginia Institute of Marine Science, Department of Aquatic Health Sciences, William & Mary, Gloucester Point, VA 23062

¶ Corresponding author

Patty Zwollo

Department of Biology

William and Mary

Williamsburg, VA 23185

FAX: 757-221-6483

Phone: 757-221-1969

pxzwol@wm.edu

ABSTRACT

Environmental microplastic pollution (including polystyrene, PS) may have detrimental effects on the health of aquatic organisms. Accumulation of PS microplastics has been reported to affect innate immune cells and inflammatory responses in fish. To date, knowledge on effects of microplastics on the antibody response is still very limited. Here, we investigated effects of small (0.8-20 μm) PS microplastics on the abundance of B lineage cells in primary cultures of developing immune cells from the anterior kidney of rainbow trout. Both purchased PS microbeads and PS microparticles generated from consumer products were used as microplastic sources. We first show that rainbow trout phagocytic B cells efficiently took up small (0.83-3.1μm) PS microbeads within hours of exposure. In addition, our data revealed that PS microplastic exposure most significantly decreased the abundance of a population of non-phagocytic developing B cells, using both flow cytometry and RT-qPCR. PS microplastics-induced loss of developing B cells further correlated with reduced gene expression of RAG1 and the membrane form of immunoglobulin heavy chains mu and tau. Based on the induced loss of developing B cells observed in our *in vitro* studies, we speculate that *in vivo*, chronic PS microplastic-exposure may lead to suboptimal IgM/IgT levels in response to pathogens in teleost species. Considering the highly conserved nature of vertebrate B lymphopoiesis it is likely that PS microplastics will similarly reduce antibody responses in higher vertebrate species, including humans. Further, RAG1 provides an effective biomarker to determine effects of PS microplastics on B cell development in teleost species.

INTRODUCTION

The rapid global increase in plastic use and production has lead to accumulation of plastic debris in the natural environment (Jambeck et al., 2015; Borrelle et al. 2017). Plastic pollution has been documented across nearly all natural environments, with extensive research emphasis on its distribution in and impact upon freshwater and marine ecosystems (Hale et al., 2020). This debris is abrased and weathered over time in the environment, forming fragments including microplastics (1 μm – 5 mm diameter; Hartmann et al. 2019). These 'secondary microplastics' are far more abundant than manufactured primary microplastic particles (Hartmann et al., 2019; Hale et al. 2020). As the majority of plastic debris derives from single-use products, microplastic pollution is dominated by polymers therein, including polyethylene, polypropylene and polystyrene (PS) (Geyer et al. 2017; Borrelle et al. 2017). The potential impacts of these microplastics on aquatic resources have been explored, with particular emphasis on PS microplastics as they are more easily purchased as spherical microbeads in the micro and nanoplastic size range than other polymers. Accumulation of PS microplastics has been observed in fish intestines, gills and skin (Choi et al., 2018; Zitouni et al., 2020; Espinosa et al., 2018). Besides acute mortality, some exposure studies suggest that more complex impacts, including immune function, merit further investigation (Bucci et al. 2019).

Most studies investigating the immune response to microplastics have focused on innate immunity, and generally suggest that microplastic exposure has an activating role. In one study, injection of zebrafish (*Danio rerio*) larvae with 0.7 μm PS microbeads enhanced expression of complement genes and, further, led to co-localization of PS microplastics and neutrophils/macrophages (Veneman et al., 2017). Limonta et al. (2019) found increased abundance of neutrophils in gills and intestinal epithelium of zebrafish after exposure to PS microbeads and enhanced expression of Major Histo Compatibiity (MHC) Class II genes. Greven et al. (2016) noted increased neutrophil degranulation and extracellular trap release in fathead minnow (*Pimephales promelas*) after exposure to 41 nm sized PS microbeads. Hamed

et al. (2019) noticed a significant decline in monocytes in the blood of juvenile Nile tilapia (*Oreochromis niloticus*) after a 15-day exposure to irregularly-shaped PS microbeads (>0.1 μm) at concentrations of 1, 10, 100 μg/ml.

Microplastics may also have significant effects on cytokine production. For example, increased overall expression of pro-inflammatory Interleukin-1β (IL1β) was noted 24 hours after injection of 0.25 nm sized PS nanoplastics in zebrafish embryos, and similarly after waterborne exposure (Brun et al., 2018). However, Lu et al. (2018) found that expression of *il1β* genes was downregulated in rainbow trout gills after 2 hours of exposure to 1 μm sized PS microplastics. Size of PS microplastic, exposure period, and/or the target tissue likely affect the IL1β response pathway differentially. Lu et al. (2018) observed significant upregulation of the type II interferon-γ (*ifnγ)* gene in rainbow trout gills after exposure to 0.2 μm and 40 μm sized PS microbeads, and in zebrafish exposed to 1 μm and 90 μm sized PS microbeads. Prietl et al. (2014) showed that 0.1 and 1 μm sized PS microbeads induced IL-6 and IL-8 secretion in monocytes and macrophages in human cell lines and peripheral blood leukocyte (PBL) cultures. Similarly, IL-8 gene expression increased in human lung A549 epithelial cells after treatment with 64 nm sized PS microbeads after 2 hours, and treatment with 202 and 535 nm PS after 4 hours (Brown et al., 2001). Yet, in zebrafish exposed to 0.2 and 20 μm sized PS microbeads, Lu et al. (2018) reported a down-regulation of expression in the *il8* gene. Together, studies so far suggest that PS microplastics have significant dysregulating and/or pro-inflammatory effects on the innate immune system of vertebrates, including fish.

Phagocytosis may be an important pathway for the uptake of microplastics by immune cells. Teleost myeloid lineage professional phagocytes, such as macrophages and neutrophils, can rapidly phagocytose particles smaller than themselves, generally < 10 μm in diameter with maximum efficiency between 3-5 μm (Champion et al. 2008). B cells exhibit phagocytic properties as well; in rainbow trout (*Oncorhynchus* mykiss) B cells were able to engulf 0.5 to 2

103 μm sized particles *in vivo* and *in vitro* (Li et al., 2006). However, fewer studies have focused on
104 this aspect of immunity in response to microplastic pollution.
105 Despite extensive research on the innate immune system, very little is known about effects
106 of PS microplastics on B-cell development. In teleost fishes, immune cells are generated in the
107 anterior kidney through B lymphopoiesis. Various B lineage cell populations at this
108 hematopoietic site have been defined by flow cytometric and quantitative polymerase chain
109 reaction (qPCR) analyses (Zwollo, 2011; Moore et al., 2019). Developing B cells co-express B-
110 cell specific transcription factor Pax5 and recombination activating gene (RAG1; Zwollo et al.,
111 2010), but have low expression of the membrane-bound form of immunoglobulin (Ig) mu (IgM)
112 or tau (IgT; Zwollo et al., 2008; Zwollo et al., 2017). In contrast, immature and mature B cells
113 co-express Pax5 and membrane-bound IgM or IgT, but not RAG1 (Zwollo et al., 2008; Zwollo et
114 al, 2017). IgM is the most prevalent systemic Ig, while IgT plays essential roles in mucosal
115 immunity and microbiota homeostasis (Hansen et al., 2005) (Salinas et al., 2011) (Xu et al.,
116 2020). Our group has also reported on an early developing B cell population which co-
117 expresses Pax5, IL1β, and a marker recognized by the myeloid/granulocyte antibody Q4E
118 (MacMurray et al., 2013; Moore et al., 2019). A summary of these cellular phenotypes based on
119 these markers is listed in Table I.
120 Existing work motivates further research regarding B cell response to microplastics.
121 Rubio et al. (2020) exposed a human B cell line to 50nm PS microbeads and found
122 compromised cell viability after 24- and 48-hour exposure *in vitro*. A recent report by Gu et al.
123 (2020) found that exposure of zebrafish intestinal cell cultures to PS microbeads induced down-
124 regulation of genes within the immune network for Ig Z/tau production, using single cell RNA-
125 sequencing; this suggests that PS microbeads disrupt the mucosal antibody response. In
126 contrast, exposure to 1 μm PS microbeads *in vivo* resulted in upregulation of the Ig heavy chain
127 mu (HCmu) gene after a short (2-hour) exposure in gills of zebrafish but not rainbow trout (Lu et

al., 2018). And, again, B cells have been noted to phagocytize PS microparticles (Li et al., 2006).

Here, we investigated *in vitro* effects of small (0.8-20 μm) PS microplastics on B cell populations in anterior kidney cultures of rainbow trout. Two forms of PS microplastics were used: purchased PS microbeads (perfectly spherical particles, commonly used in studies on phagocytosis of immune cells) and PS microparticles generated from consumer products (irregularly shaped, akin to most microplastics in the environment). Hereafter, these will be distinguished as PS microbeads and PS microparticles, respectively, or cumulatively as PS microplastics. Based on published work (Li et al. 2006), we predicted that phagocytic B cells would preferentially take up small PS microplastics (1-2 μm). Further, we hypothesized that the main effects of PS microplastics would be a consequence of phagocytosis, resulting in reduced cell viability and/or apoptosis of B cells. However, our results revealed that PS microplastic exposure most significantly affected a population of Pax5 and RAG1 co-expressing ($Pax5^+/RAG1^+$) non-phagocytic developing B cells. This result was further supported by gene expression analyses targeting immune-related genes. Together, our data reveal a dose- and size-dependent *decrease* in developing B cells after exposure to PS microplastics in culture. We propose that this may ultimately result in suboptimal humoral immune responses to pathogens in PS microplastic-exposed fish.

METHODS

Cell lines

The carp macrophage cell line CLC (European Collection of Cell Cultures # 95070628) was grown according to instructions, as follows: DMEM medium with 2mM Glutamine, 1% non-essential amino acids, 50 μg/ml gentamycin, and 10% heat-inactivated fetal bovine serum (FBS).

Rainbow trout cells and primary cultures

Naïve rainbow trout (30-75 grams) were euthanized and white blood cells (wbc) from the anterior kidney isolated through a Histopaque density gradient, as described previously (Zwollo et al., 2008). The cell yield after Histopaque purification was typically between 0.2 – 2 x 10^7 cells per fish, providing sufficient purified anterior kidney wbcs for one type of experiment, either flow cytometry or gene expression. Wbcs were cultured in trout culture medium (TCM) in the presence of LPS (*F. psychrophilum* strain CSF259-93) at 50 µg/ml at 10^7 cells/ml at 18˚C and in the presence of blood gas (10% CO_2, 10% O_2, 80% N_2) as described elsewhere (Zwollo et al., 2015), Yui and Kaattari 1987*)*. Cells were fed after 48 hours with one tenth of the culture volume of a 10x tissue culture cocktail (Zwollo et al., 2008) containing 500 µg/ml gentamycin, 10x essential aas, 10x non-essential aas, 70 mM L-glutamine, 70 mg/ml dextrose, 10x nucleosides, and 33% FBS.

Polystyrene microparticles

Biotinylated PS microbeads were purchased from Spherotech Inc. in four sizes: 0.83 µm (range 0.7-0.9 µm), 3.1 µm (range 3.0-3.9 µm), 6.8 µm (range 6.0-8.0 µm), and 16.5 µm (range 13.0-17.9 µm). Stock solutions of beads were made to 5 mg/ml in phosphate-buffered saline (PBS; 0.137 M NaCl, 0.0027 M KLC, 0.01 M Na_2HPO_4, and 0.0018 M KH_2PO_4, pH 7.4), containing 0.02% sodium azide (PBSA). 10-fold serial dilutions were made from the stock solutions in sterile PBSA in the range of 0.01-100 µg/ml. PS microbeads were vortexed for 30 seconds immediately before adding to cell cultures.

For some of the experiments, the total volume of PS microbeads added to each culture was calculated (independent of particle size) considering a PS density of 1.05 g/ml: 0.1 µg/ml of PS beads have a volume of 9.5^10^{-8} cm^3, 1 µg/ml of PS beads have a volume of 9.5^10^{-7} cm^3, 1 µg/ml of PS beads have a volume of 9.5^10^{-7} cm^3 ,10 µg/ml of PS beads have a volume of 9.5^10^{-6} cm^3, and 100 µg/ml pf PS beads have a volume of 9.5^10^{-5} cm^3.

Expanded PS packaging material (a common form of single-use containers) was used to create irregularly shaped PS microparticles, generated via cryogenic grinding (Retzch CryoMill) and sieving with a 20 μm tapper sieve, as in Seeley et al., 2020. The resulting material ranged from ~1-40 μm, with 50% of particles being ≤16 μm (size distribution and image: Supplementary Figure 1). The same concentrations were used in these experiments as the purchased PS microbeads experiments. PS particles were serially diluted 10-fold in RPMI1640 medium containing 10% FBS (Thermofisher SCI) to generate single-particle suspensions. A control cocktail of biotinylated PS microbeads was made to mimic the size distribution of the irregularly shaped PS microparticles (Supplementary Figure 1) and contained 0.1% 0.83 μm particles: 4% 3.1 μm particles: 28% 6.8 μm size particles, and 68% 16.5 μm particles.

For cell line cultures or anterior kidney primary cell cultures, various types and sizes of PS microplastics in concentrations ranging from 0-100 μg/ml were added immediately after plating the cells, followed by gentle resuspension. After incubation with PS microplastics was complete, cells were collected for fixing (see below) or alternatively, cells were spun at 400 g for 10 minutes, cell pellets resuspended in 1 ml RNazol-RT (Molecular Research Center, Inc), and stored at -80˚C until RNA extraction.

Antibodies

The monoclonal mouse anti-trout immunoglobulin heavy chain mu (HCmu, or I-14; (DeLuca, 1983) was a gift from Dr. Greg Warr. The monoclonal mouse anti-trout immunoglobulin tau antibody (41.8; (Zhang et al., 2010) recognizes IgT1, IgT2, and IgT3 (Zhang et al., 2017) and was a gift from Dr. Oriol Sunyer. The rabbit polyclonal Pax5 antibody (previously called ED-1; (Zwollo et al., 2008) recognizes the paired domain of vertebrate Pax5 and detects trout Pax5 in pre-B through plasmablast stages (MacMurray et al., 2013). The rabbit polyclonal RAG1 antibody (H300; recognizing amino-acids 744-1043 of the human RAG protein) was purchased from Santa Cruz Biotech, and has been used in previous studies

(Zwollo, et al 2010). The Q4E monoclonal antibody was a gift from Drs. Kuroda and Dr. Bernd Kollner (Friedrich-Loeffler Institute, Federal Research Institute, Germany), and recognizes rainbow trout granulocytes, monocytes and macrophages, but not resting mature lymphocytes or thrombocytes (Kuroda et al., 2000). Isotype control antibodies included rabbit IgG or mouse IgG (eBiosciences) conjugated to Alexa Fluor 555 or Alexa Fluor 647. All antibodies were aliquoted and stored in 1% BSA at −20°C.

Cell collection, fixation, and flow cytometry

Before collecting cells for fixing, images of the cultures in the culture plates were made on a phase-contrast microscope with a LabCam Microscope Adaptor for iPhone 7/8 (iDu Optics). Collected cells were fixed in 1% ice-cold paraformaldehyde (10% stock, EM-grade; Electron Microscopy Sciences) and permeabilized in 1 mL ice-cold 80% methanol, as described previously (Zwollo et al., 2010). After overnight incubation at -20°C, cells were either resuspended in permeabilizing solution (BD perm wash in PBS, BD Biosciences) and stained as described previously, or refixed for long-term storage at -80˚C in FBS containing 10% DMSO (Zwollo et al., 2010; MacMurray 2013). Percentages of cells with phagocytosed particles were monitored using streptavidin-APC750 (1:1500; Thermofisher SCI.) prior to antibody staining. Approximately 30,000 events were acquired per sample using a BD FACSArray (BD Biosciences). Duplicate samples for each staining combo were run for each experiment. Contour graphs were generated using WinMDI 2-8 (J. Trotter 1993–1998) software.

Proliferation and cell viability.

Cell proliferation rates were determined using a Click-it kit (Thermofisher SCI.) in combination with antibody staining and followed by flow cytometric analysis, as described previously (Barr et al., 2011). Cell viability was determined using the fixable viability staining kit

Live-or-Dye 564/583, following the manufacturer's instructions (Biotium), and was followed by antibody staining and flow cytometric analysis.

RNA Extraction, cDNA synthesis, and qPCR.

Total RNA in RNAzol RT (Molecular Research Center, Inc) was purified according to manufacturer's instructions. RNA concentration was measured using a Nanodrop ND-1000 Spectrophotometer (Thermofisher SCI.) and RNA stored at -80°C for future use. cDNA was synthesized using iScript™ Reverse Transcriptase Supermix for RT-qPCR, using random primers (Bio-Rad Laboratories, Inc.). Quantitative real-time PCR to determine expression of memHCmu, secHCmu, memHCtau, secHCtau and a-tubulin have been described previously (Chappell et al., 2017; Quddos and Zwollo, 2021). A custom RAG1 Taqman probe was developed by Thermofisher SCI. Forward primer: 5'-GCG CTG CTG GAC ATTGG-3', reverse primer: 5'-GGT CTC CAC CCA GGG ACA T, and reporter 5'-CAG CTT CTC CAG GAC CC-3. All qPCR assays were performed using a StepOne Real-Time PCR instrument (Applied Biosystems Inc). Average CT scores from triplicate samples were determined for each target gene. Fold change (RFC) was determined by subtracting the delta [$CT(target_{ref})$-$CT(tubulin_{ref})$] of a control fish from the delta[$CT(target_{sample})$-$CT(tubulin_{sample})$] of each sample to obtain ddCT, and 2^-ddCT calculated for each sample. Relative fold-change was calculated by normalizing the "no bead" values to 100%.

RESULTS

Phagocytosis in a teleost macrophage cell line

Initially, patterns of phagocytosis were investigated using a fish cell line, carp macrophage cell line CLC. Cells were exposed to four sizes of PS microbeads (0.83 µm, 3.1 µm, 6.8 µm, and 16.5 µm) under varying particle concentrations (0, 0.01, 0.1, 1, 10, and 100 µg/ml). The PS microbeads contained a biotin conjugate to enable intracellular detection using

fluorochrome SA-APC750. The smallest size (0.83 μm) was selected because it most closely mimics the size of bacterial particles. The largest size (16.5 μm) was selected to measure effects on cells independent of phagocytosis. PS microbead uptake was measured as early as 2 hours after exposure, but uptake was highest after 16 hours, and returned to background levels after 3 days.

As expected, cellular exposure to higher concentrations of PS microbeads resulted in a higher percentage of cells that had phagocytosed PS microbeads (Figure 1A). Smaller PS microbeads were taken up more frequently than larger sizes: at 100 μg/ml concentrations of beads, 60.7% +/- 6.6 of the cells (using 0.83 μm size PS), 5.96 % +/- 2.66 of the cells (using 3.1 μm PS), 15.2% +/- 1.82% of the cells (for 6.8 μm PS), and 3.48% +/- 1.24% of the cells (for 16.5 μm PS.

To rule out effects from non-specific binding (e.g., by PS microbeads adhering to the cell surface), a negative control sample was included: CLC cells were combined with 100 μg/ml PS microbeads (for each size) and processed immediately. The percentage of nonspecific binding was not significantly different from the negative controls (not shown), supporting that the measured percentage of APC-750-positive cells reflects the level of phagocytosis in the test samples.

Phagocytosis of PS microplastics could potentially be expected to increase cell death, especially based on our observation that phagocytosis-positive cells were lacking after 3 days. However, no significant differences in viability were observed within the time period studied.

Phagocytosis by trout immune cells.

To identify immune cell populations that have the ability to phagocytose PS microbeads in fish, purified wbcs from the anterior kidney of rainbow trout were cultured in the presence of biotinylated PS microbeads for either 16 hours or 3 days. The abundance of myeloid cells that had taken up PS microbeads was determined by 2-color flow cytometry using myeloid marker

Q4E (Moore et al, 2019), in combination with the SA-APC750 marker, as described for CLC cells.

The average abundance of APC750-positive myeloid-lineage cells ($APC750^+/Q4E^+$) was higher after 16 hours compared to after 3 days (Figure 1B, and data not shown, respectively). After 16 hours of exposure, myeloid cells phagocytosed the smallest PS microbeads most efficiently, and uptake abundance decreased as PS microbead size increased (at 100 µg/ml bead concentration: 8.73% +/- 0.93 for 0.83 µm particles, 4.06% +/- 0.64 for 3.1 µm beads, 2.96 +/- 0.47 for 6.8 µm beads, and 0.82% +/- 0.03 for 16.5 µm beads; Figure 1B). Uptake for all sizes except the largest bead sizes (16.5 µm), was significantly higher compared to the no-PS control for concentrations ≥10 ug/ml.

After a 3-day exposure, only the highest PS microbeads concentration (100 µg/ml) showed a significant increase in $APC750^+$ cells as compared to no beads, and only when using the smallest bead size (0.83 µm; data not shown). From these data, it follows that rainbow trout myeloid lineage ($Q4E^+$) cells can take up significant amounts of PS microbeads after exposure for 16 hours, and that the abundance of cells with phagocytosed beads decreases significantly after this time, as was also seen for the CLC cell line. To determine whether PS microbeads effected viability of phagocytic cells, we used the Live-or-Dye PE assay. However, we did not detect any significant differences in cell death between samples for the time periods studied.

To investigate effects of PS microplastics on phagocytic B cells, we used B cell marker Pax5 together with the SA-APC750 reagent in a flow cytometric approach. Results showed that B cells took up the smallest (0.83 µm) PS beads most efficiently, compared to the three larger sizes (Figure 2A). When using 0.83 µm sized PS beads at 100 µg/ml, the average percentage of $APC750^+/Pax5^+$ cells was 15.1% +/- 0.57 after 16 hours incubation (Figure 2A), but abundance was reduced to 3.4% +/- 0.27 after 3 days (data not shown). This pattern of reduced abundance of phagocytosis-positive B cells over time was similar to what was observed for rainbow trout myeloid cells and the carp macrophage cell line.

B cells ($Pax5^+$) were significantly more efficient at taking up 0.83 μm beads than non-B cells ($Pax5^-$ cells; Figure 2B). For 6.8 μm PS microbeads, the opposite pattern was observed; more $Pax5^-$ (non-B) cells took up 6.8 μm beads compared to $Pax5^+$ cells (Figure 2B). As expected, very few cells took up the 16.5 μm beads (the size of these PS microbeads is ≥ the size of the average immune cell), and this pattern was similar for both $Pax5^+$ and $Pax5^-$ cells (Figure 2B). No effect of microbeads on cell viability was observed for any bead size, time of exposure, or concentration, using the Live-or-Dye dye (results not shown).

In conclusion, both myeloid and B cell populations were able to phagocytose PS microbeads, with the 0.83 μm beads being more efficiently phagocytosed by B cells compared to myeloid cells, and vice-versa for the 6.8 μm beads. As expected, phagocytosis by 16.5μm PS beads size was very low, independent of cell type.

Changes in abundance of immune populations after exposure to PS microbeads

Next, possible changes in cell abundance were determined for B and myeloid cells, using the same markers, Q4E and Pax5. No significant changes in abundance of myeloid-lineage ($Q4E^+/Pax5^-$) cells were detected after 16 hours or 3 days of particle exposure, independent of particle size or concentration (data not shown). In contrast, a moderate but significant size- and concentration-dependent decrease in B cell ($Q4E^-/Pax5^+$) abundance was first detected after 16 hours (data not shown) and more significantly so after 3 days (Figure 3A).

Interestingly, a strong and dose-dependent reduction in cell abundance was seen for a subpopulation of Pax5-positive B cells that expressed Q4E (phenotype $Q4E^+/Pax5^+$). Previously, we had suggested that this population represents o population of early developing B cells (MacMurray et al., 2013; Moore et al., 2019). Using three-color flow cytometry, we found that $Q4E^+/Pax5^+$ cells were almost exclusively APC750-negative, hence $Q4E^+/Pax5^+$ cells were

not phagocytic (data not shown). This result also supports our earlier data that phagocytic $Q4E^+$ cells (Figure 1B) represented myeloid cells, not developing B cells.

To provide further evidence that $Q4E^+/Pax5^+$ cells were developing B cells, we used marker RAG1, which is expressed in developing B cells during immunoglobulin gene rearrangement (Zwollo et al, 2010). Results showed that that majority of $Q4E^+/Pax5^+$ cells stained positive for RAG1, confirming their developing B cell status. We focused our remaining experiments on this population of developing B cells, defined as $Q4E^+/Pax5^+/RAG^+$ cells. Dose-dependent effects of PS microbeads on developing B cells were observed after 16 hours exposure (data not shown), but were stronger after 3 days, and seen for all four particle sizes (Figure 3B). The reduction in developing B cell abundance was seen both in *larger* particles and in *smaller* particles (Figure 3B), further supporting the thesis that this effect is likely independent of phagocytosis.

Effect of PS microplastic size on abundance of developing B cells

Unexpectedly, we also observed a *particle size-dependent* reduction in the developing B cell population. By comparing the change in abundance of developing B cells based on *volume* of PS added for each bead size, we found a very strong correlation for the smallest beads (0.83 μm; R^2=0.995), with a higher volume of PS beads added correlating with lower abundance of developing B cells. However, only a weak correlation was seen using the largest microbeads (16.5μm, R^2= 0.245). A scatter plot of the results for all four bead sizes is shown in Figure 4, and suggest that addition of the large (16.5 μm) PS beads may affect developing B cells differently compared to smaller beads.

Changes in immune populations after exposure to irregularly shaped PS microparticles.

To further examine effects of PS microplastics on B cells, irregularly shaped PS microparticles were generated to more closely mimic the *in vivo* situation of PS microplastics

present in the aqueous environment of salmonid species. As a control, we prepared a similar size distribution of the PS microbeads to what we had used previously (0.1% 0.83 μm beads: 4% 3.1 μm beads: 28% 6.8 μm beads, and 68% 16.5 μm beads) for comparison. Anterior kidney cell cultures were exposed to the two PS cocktails (microparticles and microbeads) for 3 days. This exposure period was chosen based on data (above) showing its strong effects on abundance of developing B cells (see Figure 3B). Interestingly, similar, significant and dose-dependent decreases in developing B cells were observed for both the PS microparticles and the control microbead cocktail (Figure 5A).

Next, we determined the strength of correlation between volume of added PS microparticles and abundance of developing B cells, as was done for the PS microbeads. Interestingly, the strength of correlation for PS microparticles (R^2=0.545) was higher than for the large (16.5 μm) microbeads (R^2= 0.245), but lower than for the small (0.83, 3.1, and 6.8 μm) microbeads (R^2=0.995-0.865; see Figure 4). This is in agreement with the hypothesis that larger (~16 μm) microplastic sizes may affect developing B cells differently than smaller PS particles.

An interesting pattern of non-random distribution of particles was observed using the microscope: In the *absence* of microplastics, clusters of (dividing) cells normally form in the tissue culture dish, and presumably represent dividing cells (Supplemental Figure 2A). Interestingly, added microplastics were found to have strongly co-localized within these cell clusters, both for the 16.5 μm PS microbeads (Suppl. Figure 2B) and for the PS microparticles (Suppl Figure 2C). The co-localization pattern was visible for both 16 hours and 3-day incubation periods. The basis for this pattern remains unclear.

RAG1 and Ig as markers for PS-sensitive immune cells

To determine whether Ig-expressing B lineage cells were affected by the PS microparticles, flow cytometry was performed using either the IgM or IgT marker, in combination with RAG1. Three populations of B cells can be detected using these two markers: 1) Early

385 developing B cell populations, which express RAG1, but not yet the heavy chain for IgM (HCmu)
386 or IgT (HCtau) (phenotype $mu^{-}/tau^{-}/RAG1^{+}$), 2) An intermediate stage of developing B cells that
387 co-express RAG1 with mu or tau (phenotypes $mu^{+}/RAG1^{+}$ or $tau^{+}/RAG1^{+}$), and 3) Late
388 developing B cells, which express HCmu or HCtau, but no longer express RAG1 (phenotypes
389 $mu^{+}/RAG1^{-}$ or $tau^{+}/RAG1^{-}$; see Table I). Results show that three RAG1-expressing populations
390 ($mu^{-}/RAG1^{+}$, $tau^{-}/RAG1^{+}$, and $mu^{+}/RAG1^{+}$) had reduced cell abundance in the presence of PS
391 microparticles, while late developing B cell populations ($mu^{+}/RAG1^{-}$ and $tau^{+}/RAG1^{-}$) did not
392 (Figure 5B, 5C). Further, $tau^{+}/RAG1^{+}$ cell abundance was also not significantly changed by PS
393 microparticles (Figure 5C).
394 Together, these flow cytometric experiments show that irregularly shaped PS
395 microparticles, like PS microbeads, affected a population of Ig-negative, $RAG1^{+}$ B cells, while
396 late developing B cells ($RAG1^{-}$) of either isotype (IgM / IgT) were not affected.
397
398 **Effects of PS microparticles on cell proliferation and viability of developing B cells.**
399 Next, we determined whether or not PS microparticles affected the viability of developing
400 B cells, using the Live-or-Dye PE assay. Results showed that the percentage of dead or dying
401 $RAG1^{+}$ cells (prior to fixing) was not affected by the presence of PS microparticles after 3 days
402 (Figure 6A; ($RAG1^{+}/PE^{+}$). In contrast, the percentage of “non-dying” ($RAG1^{+}/PE^{-}$) cells
403 *decreased* significantly between samples not exposed to particles compared to cells exposed to
404 1 and 10 µg/ml of PS microparticles (Figure 6A). Hence, the observed reduction in abundance
405 of developing B cells in the presence of PS microparticles was not caused by increased cell
406 death.
407 Next, to determine whether PS microparticles affected the proliferation of developing B
408 cells, we used Edu/Click-iT assays to measure proliferating cells in combination with RAG1
409 expression in two-color flow cytometry, and measured effects after 3 days. No significant
410 changes in the abundance of either proliferating ($RAG1^{+}/Edu^{+}$) or non-proliferating ($RAG1^{+}/Edu^{-}$

411) cells were observed when comparing exposure to 0, 1, and 1 µg/ml of PS particles (results not
412 shown).
413
414 **PS-induced changes in immune gene expression.**
415 To determine if the reduced cellular abundance of developing B cells after PS exposure
416 correlated with a reduction in RAG1 gene expression, we developed a Taqman RT-qPCR
417 assay. Data show a significant reduction in expression of RAG1 after 3 days exposure to 1 or 10
418 µg/ml PS microparticles (Figure 6B).
419 Next, we measured effects of PS microparticles exposure on Ig expression, using the
420 same samples as used for RAG1 expression assays. We measured levels of membrane-bound
421 HCmu (memHCmu) and membrane-bound HCtau (memHCtau). Results showed a dose-
422 dependent decrease in expression of both targets in the presence of 1 or 10 µg/ml of PS
423 microparticles (Figure 6B). Hence the average expression of all three target genes was reduced
424 after 3 days of exposure to PS microparticles.
425
426 **DISCUSSION**
427 Here we report on the inhibiting effects of PS microplastics on the abundance of rainbow
428 trout B lineage cells in culture. Our data suggest that PS microplastics have at least two
429 different effects: efficient phagocytosis of small (0.83 µm) PS microplastics by B cells, and
430 dysregulation of B cell development independent of phagocytosis by larger (16.5 µm) PS
431 microplastics.
432
433 **Phagocytosis of microplastics.**
434 Phagocytosis occurred in both myeloid and B lymphoid cells and was dose-dependent
435 for both cell lineages. Both myeloid and B lineage cells took up the smallest beads most
436 efficiently, in agreement with earlier reports in rats and mice. Champion et al. (2008) reported on

437 the significance of particle size in phagocytosis of polymeric microspheres in rat alveolar
438 macrophages and found maximum phagocytosis for particles of 2-3 μm. The authors suggest
439 that the recognition of this size range is highly conserved, as pathogen clearance is a major
440 function of macrophages. The 2-3 μm size range optimum seems to be conserved in rainbow
441 trout, which reportedly phagocytosed 2.8 μm protein-coated particles within hours after
442 exposure, mostly though scavenger receptors on macrophages (Frøystad et al., 1998).
443 The phagocytic nature of B cells has been studied in rainbow trout, and these (B1-like) B
444 cells preferentially take up particles ≤2 μm (Li et al., 2006). Phagocytic B cells are mostly small
445 (~6 μm) cells at the *mature* B cell stage (Wu et al., 2019) supporting our conclusions that
446 *developing* B cells are not capable of phagocytosing PS microplastics. Importantly, our results
447 show that mature B cells were even more efficient at taking up 0.83 μm PS beads compared to
448 myeloid cells in rainbow trout. In agreement with our findings, Overland et al. (2010) reported
449 that Atlantic salmon B cells had a higher phagocytic ability for 1 μm latex beads compared to
450 neutrophils, in anterior kidney cultures (but not in blood).
451 The vulnerability of B cells to microplastics suggested by our findings that these cells
452 were able to phagocytose small (0.83 μm) PS microbeads with high efficiency. Although we
453 were unable to measure significant loss of cell viability within the 3-day time frame, others have
454 shown that phagocytosed PS microplastics (0.1-5 μm) increased ROS levels in phagocytic cells,
455 and size-dependent induction of apoptosis (Wu et al, 2019; Hu and Palic, 2020). As such, we
456 predict that microplastics may interfere with the critical role of pathogen clearance by phagocytic
457 B cells, especially from chronic exposure *in vivo*.
458
459 **How do PS microplastics affect developing B cells?**
460 Our data revealed significant dose-dependent effects of PS-microplastics on developing
461 B cells. Although little is known about how cell-cell interactions drive B cell development in
462 teleosts, detailed information is available from mouse studies. Rolink et al., (2000) developed *in*

vitro co-culture systems to decipher B cell differentiation in mouse bone marrow (the functional equivalent of teleost anterior kidney). They demonstrated that developing B cells (progenitors and pre-BI cells) will maintain long-term proliferation in culture when in the presence of Interleukin 7 (IL7)-expressing stromal cells. Removal of stromal cells (and IL7) induced differentiation into immature B IgM^+ cells, with direct cell-cell contact between IL7-expressing stromal cells and IL7 receptor-positive developing B cells being essential for this process (Rolink et al., 2000; Aurrand-Lions and Mancini, 2018; Gauthier et al., 2002; Patton et al., 2014). Hence, prevention of these essential interactions will stop cell-division, and prematurely drive differentiation towards more mature B cells. Similar cell-cell dependent maturation mechanisms are likely present in the anterior kidney in teleost species.

We propose that in our experimental system, PS microplastics interfered with cell-cell interactions between stromal cells and proliferating RAG^+ B cells, which drove accelerated differentiation towards $RAG1^-$ negative, more mature B cells. This hypothesis, illustrated in Figure 7, would explain the observed reduction in abundance of RAG^+ developing B cells in microplasics-exposed cultures. It is also supported by the observed reduction in gene expression for RAG1, HCmu, and HCtau, in PS-exposed cells. However, the lack of measurable change in cell proliferation of developing B cells does not fit the model. It is possible that cell proliferation changes occur earlier during the exposure period (we only measured changes during the last 16 hours of the 3-day exposure), or that the change was too small to be significant. In support of an inhibiting effect on the net-production of developing B cells (either because they divide slower, or because they differentiate faster), a significant decrease in the percentage of live ($RAG1^+/PE^-$) cells was observed after exposure to PS microparticles: it suggests that fewer such cells were present under these conditions.

Flow cytometric analysis detected a reduced abundance of $RAG1^+$ populations (either cells co-expressing HCmu, or without HCmu) after PS microplastics exposure. This suggests that the observed reduction in memHCmu and memHCtau gene expression detected by qPCR

was caused by a reduced abundance of early developing B cells (which still express RAG1), but not of late developing/immature B cells (which lack RAG1). *In vivo*, this could in turn lead to fewer mature B cells capable of responding to pathogen. Hence, it can be argued that PS microplastics lead to reduced numbers of mature B cells, a compressed B cell repertoire, and consequently, a reduced and less diverse antibody response, and increased risk of infectious disease. This is not only inferred for trout (studied here) and other teleosts, but may also be translatable to human immune response, warranting further research as microplastic pollution is particularly abundant in indoor air and dust (Hale et al., 2020).

Larger PS microbeads showed a weaker correlation between abundance of developing B cells and volume of beads added, compared to smaller beads. This suggests that larger particles behave differently than smaller particles in their ability to interfere with B cell development. We propose that larger (>6.8 μm) microplastics are better at dysregulating B cell development through interference in cell-cell interactions, compared to smaller particles, as their larger size may result in greater steric hindrance (compare Figure 7B and 7C).

Alternatively, larger particles may be more disruptive to the organization of niche structures, highly structured locations where developing B cells differentiate/reside (Tokoyoda et al., 2004). The observations on the co-localization of microplastics with clusters of proliferating cells supports this model, although this theory clearly requires further investigation.

Differences between effects of microbeads versus microparticles.

The results presented here expand upon previous immune work using spherical plastic microbeads, by inclusion of fragments produced from actual post-consumer product PS products. Although the convenience of commercially available microbeads and their ability to be biotinylated for fluorescence-marker work is advantageous, their chemistries and shapes may be markedly different than secondary plastics common in the environment (Rochman et al., 2019). Indeed, many of the published studies cited use plastic microbeads to evaluate cellular

processes following exposure to pathogens and were not intended to elucidate consequences of environmental microplastic pollution. The work here illustrating similar response to primary microbeads and lab-generated secondary microparticles (with the exception of phagocytosis work, as generated particles were not biotinylated) illustrates that conclusions from previous microbead-based work may be pertinent in assessing secondary microparticle risk, at least in the case of PS beads and expanded PS foam microplastics. In addition, microparticles were not stored in preservatives, suggesting the effects of some preservatives in purchased microbeads did not have an effect on results shown here, as illustrated by other authors (Pikuda et al., 2019).

An unintended benefit of using PS microparticles outside of the phagocytic size range was that it revealed a novel mechanism whereby larger microplastics (10-20 μm) may interfere with cell-cell interactions essential for proliferation of developing B cells, potentially dysregulating the B cell maturation process. Further, the technique for generating and sieving plastics to reach a desirable size range (used here) should be expanded to other polymer types, including polyethylene and polypropylene, which are underrepresented in immune work despite their large contribution to environmental debris (Jacob et al., 2020).

How does this extrapolate to effects of PS microplastics in vivo?

In order to apply our *in vitro* data to predicting effects on *in vivo* exposure of PS microplastics to hematopoietic environments, one important question concerns the possible transport mechanisms of PS microplastics from mucosal areas (e.g., gills or gut) to the hematopoietic site. A number of immune cells, including macrophages, neutrophils, dendritic cells and B cells, are able to phagocytose small microplastics very efficiently (reviewed in Gustafson et al., 2015) and there is evidence that they take up PS particles from the blood or tissues. Because these cells are in the circulation, they can deliver PS microplastics to the

anterior kidney, which is a highly efficient site to clear particulate matter from the blood of fish (Moore et al., 1998).

The size thresholds limiting microplastic phagocytosis need further investigation. In mice, the upper particle limit for phagocytosis is surprisingly high: bone-marrow derived macrophages (which measure 13.8+/-2.3 µm) could phagocytose latex beads greater than 20 µm, but the ingestion of beads ≥15 µm required IgG-opsonization (Cannon and Swanson, 1992). However, it is generally assumed that the upper threshold for phagocytosis is ≤10 µm (reviewed in Gustafson et al, 2015). The latter is in agreement with our own data, which showed that PS microplastics up to 6.8 µm could still be phagocytosed, although less efficiently, while phagocytic B cells are highly efficient at taking up smaller particles (0.83 µm), and these patterns are likely to be the same *in vivo*. It should be pointed out that although small microplastics are likely the most abundant sizes, virtually all field surveys of their presence in natural waters fail to measure particles < 20 µm (and often < 300 µm) due to sampling and detection limitations (Hale et al., 2020).

In conclusion, in our study we provide evidence of a potentially detrimental effect of PS microplastics on B cell development, using a primary cell culture system. Our data provide a model to focus future *in vivo* studies on the dysregulating effects of PS microplastics on B cell developmental pathways in primary immune organs of fish and humans.

ACKNOWLEDGEMENTS. The authors wish to thank Mss. Hannah Brown and Barb Rutan, and Dr. Andrew Wargo for providing rainbow trout. Funding was through a grant from NOAA-Marine Debris Program NA19NOS9990085. Student research support was generously provided by the Freeman Family Foundation.

FIGURE LEGENDS

Figure 1. Percentage of cells with phagocytosed PS microbeads after 16 hours of exposure. Concentrations (0-100 µg/ml) for each bead size (0.83-16.5 µm) on X-axis. PS microbeads 0.83µm (white), 3.1µm (light grey), 6.8µm (dark grey), and 16.5µm (black), * p≤0.05, **p≤0.01, ***p≤0.001. **A.** Carp macrophage cell line CLC. Average percentage of $APC750^+$ cells +/– standard error (n = 4) is shown in log-scale on the Y-axis. **B**. Rainbow trout anterior kidney cells. Average percentage of $APC750^+/Q4E^+$ cells +/– standard error (n = 4) is shown in log-scale on the Y-axis.

Figure 2. Average abundance of phagocytosis (in percentages) after 16 hours of PS-microbead exposure, in rainbow trout cultures. **A.** $APC750^+/Pax5^+$ B cells; average +/- standard error (n=4) in log-scale, on Y-axis. Concentrations (0-100 µg/ml) for each bead size (0.83-16.5 µm) on X-axis. PS microbeads 0.83µm (white), 3.1µm (light grey), 6.8µm (dark grey), 16.5 µm (black), **B.** $APC750^+$ cells; average +/- standard error (n=4), comparing B-cells ($Pax5^+/APC750^+$; dots) to non-B cells ($Pax5^–/APC750^+$, diagonally striped), by PS particle size (in µm) on the X-axis, for 100 µg/ml PS beads. * p≤0.05, **p≤0.01, ***p≤0.001.

Figure 3. Effects of PS microbead size and concentration on cellular abundance (in percentages) of two different B lineage populations after 3 days of exposure. Average +/– standard error (n = 4) is shown on the Y-axis. Concentrations (0-100 µg/ml) for each bead size (0.83-16.5 µm) on X-axis. PS microbeads 0.83µm (white), 3.1µm (light grey), 6.8µm (dark grey), and 16.5 µm (black). * p≤0.05, **p≤0.01, ***p≤0.001. **A.** Immature/mature B cells ($Q4E^–/Pax5^+$). **B.** Developing B cells ($Q4E^+/Pax5^+/RAG1^+$).

Figure 4. Correlations between the relative abundance of developing B cells and the volume of PS microbeads added to the culture, comparing effects of 4 bead sizes. 3-day exposure to PS beads. Relative change in abundance (in percentages) of developing B cells (Y-axis) refers to

each value of abundance divided by the value for "no beads". R^2 values are shown for each correlation.

Figure 5. Flow cytometric analysis on effects of PS microparticles on developing B cell populations. Cellular abundance (in percentage, on the Y-axis) of after 3 days of exposure. Average +/- standard error. * p≤0.05, **p≤0.01, ***p≤0.001. **A.** Three-color flow cytometry; comparing effects of PS microbead control cocktail (left, blocks) to those of PS microparticles (right, dots) for different concentrations (0-100 µg/mL, X-axis). (n=6). **B** and **C**. Two-color flow cytometry; effects of PS microparticle exposure on cellular abundance of early and late developing B cell populations for 0, 1, and 10 µg/ml on the X-axis. (n=6). **B.** Using markers HCmu (mu) and RAG1 (rag), showing early (mu^-/rag^+; orange), intermediate (mu^+/rag^+; blue), and late (mu^+/rag^-; grey) developing B cells of the IgM class. **C.** Using HCtau (tau) and RAG1 (rag), showing early (tau^-/rag^+; green), intermediate (tau^+/rag^+; red), and late (tau^+/rag^-; yellow) developing B cells of the IgT class.

Figure 6. Effects of PS microparticles on viability of developing B cells and immune gene expression; 3 days of PS microparticle exposure. Average +/- standard error. * p≤0.05, **p≤0.01, ***p≤0.001. (n=6). **A**. Effects on cell viability using 2-color flow cytometry. $RAG1^+/PE^-$ cells (live cells; blue); $RAG1^+/PE^+$ cells (dead/dying cells; orange). **B.** Relative changes in gene expression of RAG1, memHCmu, and memHCtau, using RT-qPCR. Target genes are shown below the X-axis. PS microparticle concentrations 0 (white), 1 (grey), or 10 (black) µg/ml. Relative fold-change in gene expression normalized to the “no particle” (0 µg/ml) fold-change value set to 100% on the Y-axis.

Figure 7. Hypothesis: PS microplastics (in blue) interfere with (proliferation) signals (from IL7) on stromal cells (in green) to developing B cells (in orange). The proliferation signals are

indicated by a yellow arrow. In the absence of this interaction, developing B cells will start to differentiate towards immature B cells. The more microplastics are present in a culture, the less likely it is that a stromal cell will interact with a developing B cell. Consequently, on the average, developing B cells receive fewer proliferation signals, and may differentiate prematurely. **A.** In the absence of PS microplastics, IL7 normally provides a proliferation signal to the pre-B cells and this delays differentiation. **B.** Smaller PS microplastics interfere with the signal by blocking IL7 on stromal cells. **C.** Larger PS microplastics (with *the same* total volume compared to smaller particles) interfere both directly by blocking IL7 access, and indirectly through greater steric hindrance.

Supplemental Figure 1. Polystyrene particle size distribution histogram with a vertical red line at 20 µm (A) and microscope images for 4X (B) and 10X (C) magnifications.

Supplemental Figure 2. Patterns of cell clusters exposed to PS microplastics in cultures of anterior kidney cells **A**. Negative control (no beads) **B**.16.5 µm PS microbeads (10 µg/ml right image, see arrow). **C.** PS microparticles (10 µg/ml, see arrow). Size bars 100 µm**.**

REFERENCES.

Aurrand-Lions, M., and Mancini, S.J.C. (2018). Murine Bone Marrow Niches from Hematopoietic Stem Cells to B Cells. Int. J. Mol. Sci. 19.

Barr, M., Mott, K., and Zwollo, P. (2011). Defining terminally differentiating B cell populations in rainbow trout immune tissues using the transcription factor XbpI. Fish Shellfish Immunol. 31, 727–735.

Borrelle, S. B., Rochman, C. M., Liboiron, M., Bond, A. L., Lusher, A., Bradshaw, H., & Provencher, J. F. (2017). Opinion: Why we need an international agreement on marine

plastic pollution. Proceedings ofthe National Academy ofSciences, 114(38), 9994–9997. https://doi.

Bucci, K., Tulio, M. & Rochman, C. M. What is known and unknown about the effects of plastic pollution: A meta-analysis and systematic review. Ecol. Appl. 30, 1–16 (2019).

Brun, NR, Koch, BEV, Varela, M., Peijnenburg WJ, Spaink, HP, and Vijver, MG. (2018). Nanoparticles induce dermal and intestinal innate immune responses in zebrafish embryos. Envir. Sci. Nano. 5:904-916

Cannon, G.J., and Swanson, J.A. (1992). The macrophage capacity for phagocytosis. J. Cell Sci. 101 (Pt 4), 907–913.

Champion, J. A.; Walker, A.; Mitragotri, S. Role of Particle Size in Phagocytosis of Polymeric Microspheres. Pharm. Res. 2008, 25 (8), 1815–1821. .

Chappell, M.E., Epp, L., and Zwollo, P. (2017). Sockeye salmon immunoglobulin VH usage and pathogen loads differ between spawning sites. Dev. Comp. Immunol. 77, 297–306.

Choi, J. S.; Jung, Y. J.; Hong, N. H.; Hong, S. H.; Park, J. W. Toxicological Effects of Irregularly Shaped and Spherical Microplastics in a Marine Teleost, the Sheepshead Minnow (Cyprinodon Variegatus). Mar. Pollut. Bull. 2018, 129 (1), 231–240.

DeLuca, D. (1983). Lymphocyte heterogeneity in the trout, Salmo gairdineri, defined with monoclonal antibodies to IgM. Eur. J. Immunol. 173, 7317–7323.

Espinosa, C., Beltrán, J. M., Esteban, M. A., & Cuesta, A. (2018). In vitro effects of virgin microplastics on fish head-kidney leucocyte activities. Environmental Pollution, 235, 30-38.

Frøystad, M.K., Rode, M., Berg, T., and Gjøen, T. (1998). A role for scavenger receptors in phagocytosis of protein-coated particles in rainbow trout head kidney macrophages. Dev. Comp. Immunol. 22, 533–549.

Gauthier, L., Rossi, B., Roux, F., Termine, E., and Schiff, C. (2002). Galectin-1 is a stromal cell ligand of the pre-B cell receptor (BCR) implicated in synapse formation between pre-B and stromal cells and in pre-BCR triggering. Proc. Natl. Acad. Sci. U. S. A. 99, 13014–13019.

Geyer, R.; Jambeck, J. R.; Law, K. L. Production, Use, and Fate of All Plastics Ever Made. Sci. Adv. 2017, 3 (7), 25–29.

Greven, A.-C., Merk, T., Karagöz, F., Mohr, K., Klapper, M., Jovanović, B., and Palić, D. (2016). Polycarbonate and polystyrene nanoplastic particles act as stressors to the innate immune system of fathead minnow (Pimephales promelas). Environ. Toxicol. Chem. 35, 3093–3100.

Gu, W., Liu, S., Chen, L., Liu, Y., Gu, C., Ren, H. Q., & Wu, B. (2020). Single-Cell RNA Sequencing Reveals Size-Dependent Effects of Polystyrene Microplastics on Immune and Secretory Cell Populations from Zebrafish Intestines. Environ. Sci. Technol., 54(6), 3417–3427.

Gustafson, H., Holt-Casper, D, et al. Nanoparticle uptake: the phagocyte problem. Nanotoday 10; 2015. 487-510

Hale, R. C.; Seeley, M. E.; Guardia, M. J. La; Mai, L.; Zeng, E. Y. A Global Perspective on Microplastics. J. Geophys. Res. Ocean. 2020, 1–40.

Hamed, M., Soliman, H. A., Osman, A. G., & Sayed, A. E. (2019). Assessment the effect of exposure to microplastics in Nile Tilapia (Oreochromis niloticus) early juvenile: I. blood biomarkers. Chemosphere, 228, 345-350.

Hansen, J.D., Landis, E.D., and Phillips, R.B. (2005). Discovery of a unique Ig heavy-chain isotype (IgT) in rainbow trout: Implications for a distinctive B cell developmental pathway in teleost fish. Proc. Natl. Acad. Sci. U. S. A. 102, 6919–6924.

Hartmann, N. B.; Hüffer, T.; Thompson, R. C.; Hassellöv, M.; Verschoor, A.; Daugaard, A. E.; Rist, S.; Karlsson, T.; Brennholt, N.; Cole, M.; Herrling, M. P.; Hess, M. C.; Ivleva, N. P.; Lusher, A. L.; Wagner, M. Are We Speaking the Same Language? Recommendations for a Definition and Categorization Framework for Plastic Debris. Environ. Sci. Technol. 2019, 53 (3), 1039–1047.

Hu, M. and Palic, D. (2020). Micro and nano-plastics activation of oxidative and inflammatory adverse pathways. Redox Biology 37; 101620

Jacob, H., Besson, M., Swarzenski, P. W., Lecchini, D. & Metian, M. Effects of Virgin Micro- and Nanoplastics on Fish: Trends, Meta-Analysis, and Perspectives. Environ. Sci. Technol. 54, 4733–4745 (2020).

Jambeck, J.; Geyer, R.; Wilcox, C.; Siegler, T. R.; Perryman, M.; Andrady, A.; Narayan, R.; Law, K. L. Plastic Waste Inputs from Land into the Ocean. Science (80). 2015, 347 (6223), 3–6.

Kuroda, A., Okamoto, N., and Fukuda, H. (2000). Characterization of monocloanl antibodies against antigens shared with neutrophils and macrophages in rainbow trout. Fish Pathol. 35, 205–213.

Li, J., Barreda, D. R., Zhang, Y., Boshra, H., Gelman, A. E., Lapatra, S., . . . Sunyer, J. O. (2006). B lymphocytes from early vertebrates have potent phagocytic and microbicidal abilities. Nature Immunology, 7(10), 1116-1124.

Limonta, G., Mancia, A., Benkhalqui, A., Bertolucci, C., Abelli, L., Fossi, M.C., and Panti, C. (2019). Microplastics induce transcriptional changes, immune response and behavioral alterations in adult zebrafish. Sci. Rep. 9, 15775.

Lu, C., Kania, P. W., & Buchmann, K. (2018). Particle effects on fish gills: An immunogenetic approach for rainbow trout and zebrafish. Aquaculture, 484, 98-104.

MacMurray, E., Barr, M., Bruce, A., Epp, L., and Zwollo, P. (2013). Alternative splicing of the trout Pax5 gene and identification of novel B cell populations using Pax5 signatures. Dev. Comp. Immunol. 41, 270–281.

Moore, C., Hennessey, E., Smith, M., Epp, L., and Zwollo, P. (2019). Innate immune cell signatures in a BCWD-Resistant line of rainbow trout before and after in vivo challenge with Flavobacterium psychrophilum. Dev. Comp. Immunol. 90, 47–54.

Moore, J.D., Ototake, M., Nakanishi, T. 1998. Particulate antigen uptake during immersion immunisation of fish: the effectiveness of prolonged exposure and roles of skin and gill. Fish and Shellfish Immunology, 8, 393 407

Overland, H.S., Pettersen, E.F., Rønneseth, A., and Wergeland, H.I. (2010). Phagocytosis by B-cells and neutrophils in Atlantic salmon (Salmo salar L.) and Atlantic cod (Gadus morhua L.). Fish Shellfish Immunol. 28, 193–204.

727 Patton, D.T., Plumb, A.W., and Abraham, N. (2014). The survival and differentiation of pro-B
728 and pre-B cells in the bone marrow is dependent on IL-7Rα Tyr449. J. Immunol. Baltim. Md
729 1950 193, 3446–3455.

730 Pikuda, O., Xu, E. G., Berk, D. & Tufenkji, N. Toxicity Assessments of Micro- and
731 Nanoplastics Can Be Confounded by Preservatives in Commercial Formulations. Environ.
732 Sci. Technol. Lett. 6, 21–25 (2019).

733
734 Prietl, B., Meindl, C., Roblegg, E., Pieber, T.R., Lanzer, G., and Fröhlich, E. (2014). Nano-
735 sized and micro-sized polystyrene particles affect phagocyte function. Cell Biol. Toxicol. 30,
736 1–16.

737 Quddos, F., and Zwollo, P. (2021). A BCWD-Resistant line of rainbow trout is less sensitive
738 to cortisol implant-induced changes in IgM response as compared to a susceptible (control)
739 line. Dev. Comp. Immunol. 116, 103921.

740 Rochman, C. M. et al. Rethinking microplastics as a diverse contaminant suite. Environ.
741 Toxicol. Chem. 38, 703–711 (2019).

742
743 Rolink, A.G., Schaniel, C., Busslinger, M., Nutt, S.L., and Melchers, F. (2000). Fidelity and
744 infidelity in commitment to B-lymphocyte lineage development. Immunol. Rev. 175, 104–
745 111.

746 Rubio, L., Barguilla, I., Domenech, J., Marcos, R., & Hernández, A. (2020). Biological
747 effects, including oxidative stress and genotoxic damage, of polystyrene nanoparticles in
748 different human hematopoietic cell lines. Journal of Hazardous Materials, 398, 122900.

Salinas, I., Zhang, Y.-A., and Sunyer, J.O. (2011). Mucosal immunoglobulins and B cells of teleost fish. Dev. Comp. Immunol. 35, 1346–1365.

Seeley, M. E.; Song, B.; Passie, R.; Hale, R. C. Microplastics Affect Sediment Microbial Communities and Nitrogen Cycling. Nat. Commun. 2020, 11 (2372), 1–10.

Tang, H., Wu, T., Zhao, Z., & Pan, X. (2008). Effects of fish protein hydrolysate on growth performance and humoral immune response in large yellow croaker (Pseudosciaena crocea R.). Journal of Zhejiang University SCIENCE B, 9(9), 684-690.

Tokoyoda, K., Egawa, T., Sugiyama, T., Choi, B.-I., and Nagasawa, T. (2004). Cellular niches controlling B lymphocyte behavior within bone marrow during development. Immunity 20, 707–718.

Veneman, W. J., Spaink, H. P., Brun, N. R., Bosker, T., & Vijver, M. G. (2017). Pathway analysis of systemic transcriptome responses to injected polystyrene particles in zebrafish larvae. Aquatic Toxicology, 190, 112–120.

Wu, L., Kong, L., Yang, Y., Bian, X., Wu, S., Li, B., Yin, X., Mu, L., Li, J., and Ye, J. (2019). Effects of Cell Differentiation on the Phagocytic Activities of IgM+ B Cells in a Teleost Fish. Front. Immunol. 10, 2225.

Xu, Z., Takizawa, F., Casadei, E., Shibasaki, Y., Ding, Y., Sauters, T.J.C., Yu, Y., Salinas, I., and Sunyer, J.O. (2020). Specialization of mucosal immunoglobulins in pathogen control and microbiota homeostasis occurred early in vertebrate evolution. Sci. Immunol. 5, eaay3254.

Yui, M. A. and Kaattari, S. L. Vibrio anguillarum antigen stimulates mitogenesis and polyclonal activation of salmonid lymphocytes. Dev. Comp. Immunol.1987; 11: 539-549.)

771 Zhang, Y. A., I. Salinas, J. Li, D. Parra, S. Bjork, Z. Xu, S. E. LaPatra, J. Bartholomew, and
772 J. O. Sunyer. 2010. IgT, a primitive immunoglobulin class specialized in mucosal immunity.
773 Nat. Immunol. 11:827-835.

774 Zitouni, N., Bousserrhine, N., Belbekhouche, S., Missawi, O., Alphonse, V., Boughatass, I.,
775 & Banni, M. (2020). First report on the presence of small microplastics (≤ 3 μm) in tissue of
776 the commercial fish Serranus scriba (Linnaeus. 1758) from Tunisian coasts and associated
777 cellular alterations. Environmental Pollution, 263, 114576.2020.

778 Zhang, N., Zhang, X.-J., Chen, D.-D., Oriol Sunyer, J., and Zhang, Y.-A. (2017). Molecular
779 characterization and expression analysis of three subclasses of IgT in rainbow trout
780 (Oncorhynchus mykiss). Dev. Comp. Immunol. 70, 94–105.

781 Zhang, Y.-A., Salinas, I., Li, J., Parra, D., Bjork, S., Xu, Z., LaPatra, S.E., Bartholomew, J.,
782 and Sunyer, J.O. (2010). IgT, a primitive immunoglobulin class specialized in mucosal
783 immunity. Nat. Immunol. 11, 827–835.

784 Zwollo, P. (2011). Dissecting teleost B cell differentiation using transcription factors. Dev.
785 Comp. Immunol. 35, 898–905.

786 Zwollo, P., Haines, A., Rosato, P., and Gumulak-Smith, J. (2008). Molecular and cellular
787 analysis of B-cell populations in the rainbow trout using Pax5 and immunoglobulin markers.
788 Dev. Comp. Immunol. 32, 1482–1496.

789 Zwollo, P., Mott, K., and Barr, M. (2010). Comparative analyses of B cell populations in trout
790 kidney and mouse bone marrow: Establishing “B cell signatures.” Dev. Comp. Immunol. 34,
791 1291–1299.

792 Zwollo, P., Ray, J.C., Sestito, M., Kiernan, E., Wiens, G.D., Kaattari, S., StJacques, B., and
793 Epp, L. (2015). B cell signatures of BCWD-resistant and susceptible lines of rainbow trout: A
794 shift towards more EBF-expressing progenitors and fewer mature B cells in resistant
795 animals. Dev. Comp. Immunol. 48, 1–12.

796 Zwollo, P., Hennessey, E., Moore, C., Marancik, D.P., Wiens, G.D., and Epp, L. (2017). A
797 BCWD-resistant line of rainbow trout exhibits higher abundance of IgT+ B cells and heavy
798 chain tau transcripts compared to a susceptible line following challenge with Flavobacterium
799 psychrophilum. Dev. Comp. Immunol. 74, 190–199.

800
801

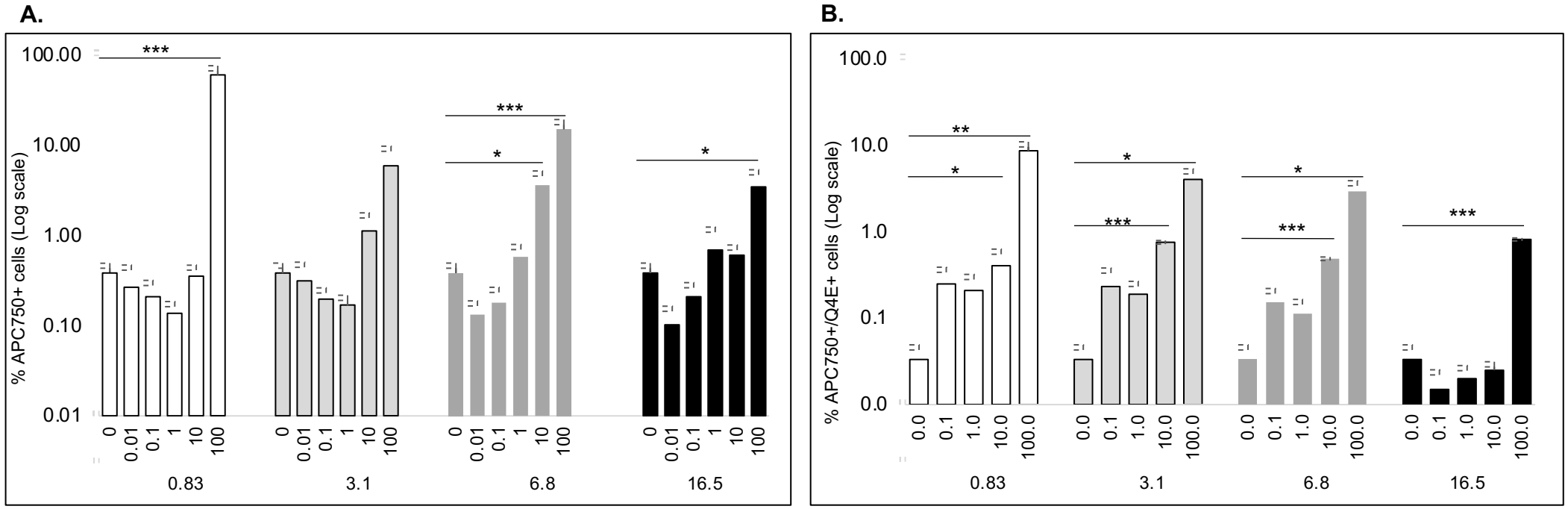
A.
B.
100.00
10.00
1.00
0.10
0.01
% APC750+ cells (Log scale)
100.0
10.0
1.0
0.1
0.0
% APC750+/Q4E+ cells (Log scale)
***
**
*
0
0.01
0.1
1
10
100
0.0
0.1
1.0
10.0
100.0
0.83
3.1
6.8
16.5

Figure 1.

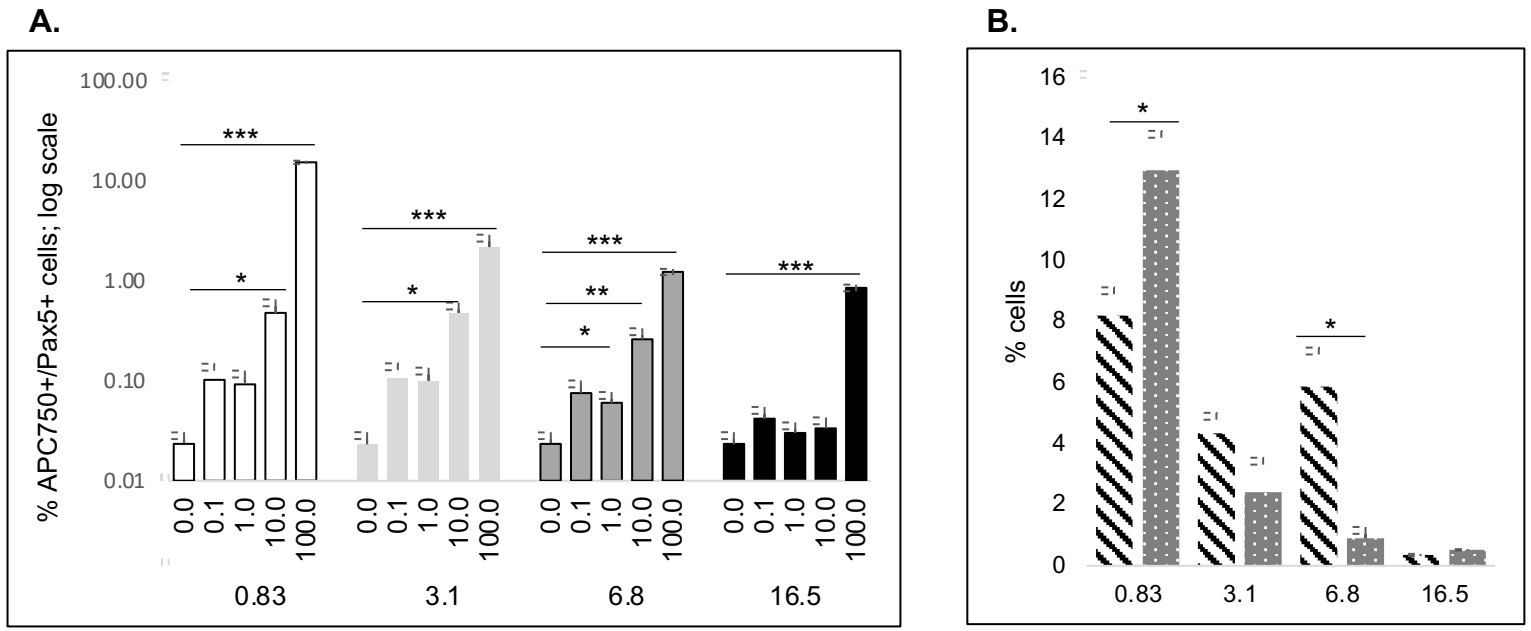
A.
B.
% APC750+/Pax5+ cells; log scale
100.00
10.00
1.00
0.10
0.01
***
*
***
*
***
**
*
***
0.0
0.1
1.0
10.0
100.0
0.83
3.1
6.8
16.5
% cells
16
14
12
10
8
6
4
2
0
*
*

Figure 2.

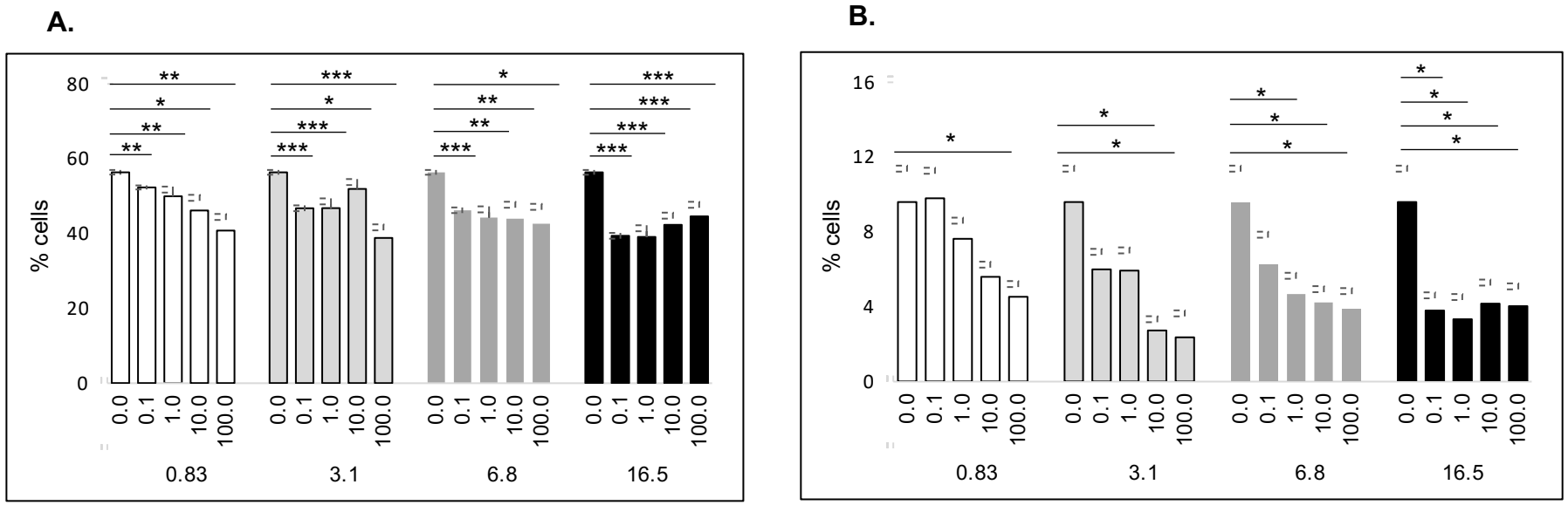

Figure 3.

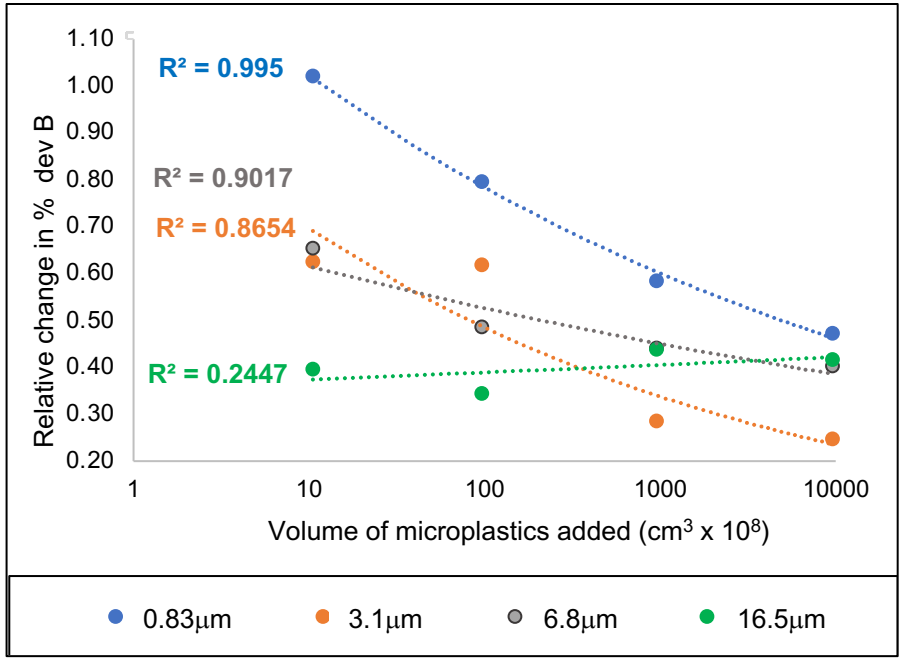
1.10
1.00
0.90
0.80
0.70
0.60
0.50
0.40
0.30
0.20
Relative change in % dev B
R² = 0.995
R² = 0.9017
R² = 0.8654
R² = 0.2447
1
10
100
1000
10000
Volume of microplastics added (cm3 x 108)
0.83µm
3.1µm
6.8µm
16.5µm

Figure 4.

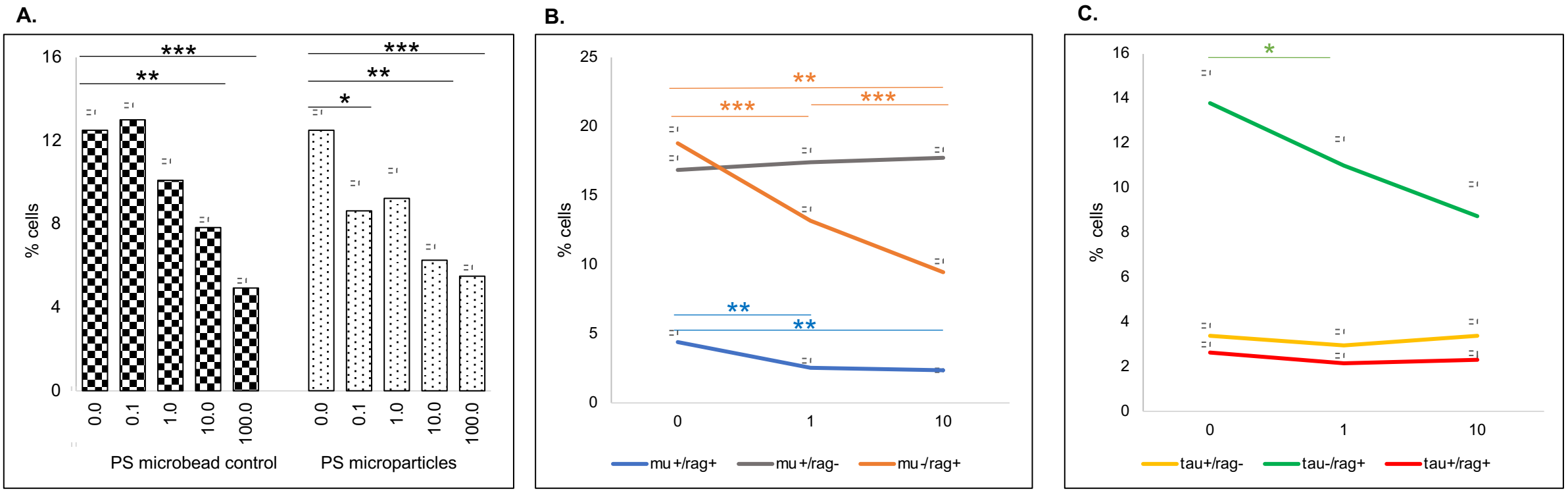
A.
16
12
8
4
0
% cells
***
**
***
**
*
0.0
0.1
1.0
10.0
100.0
0.0
0.1
1.0
10.0
100.0
PS microbead control
PS microparticles
B.
25
20
15
10
5
0
% cells
**
***
***
**
**
0
1
10
mu+/rag+
mu+/rag-
mu-/rag+
C.
16
14
12
10
8
6
4
2
0
% cells
*
0
1
10
tau+/rag-
tau-/rag+
tau+/rag+

Figure 5.

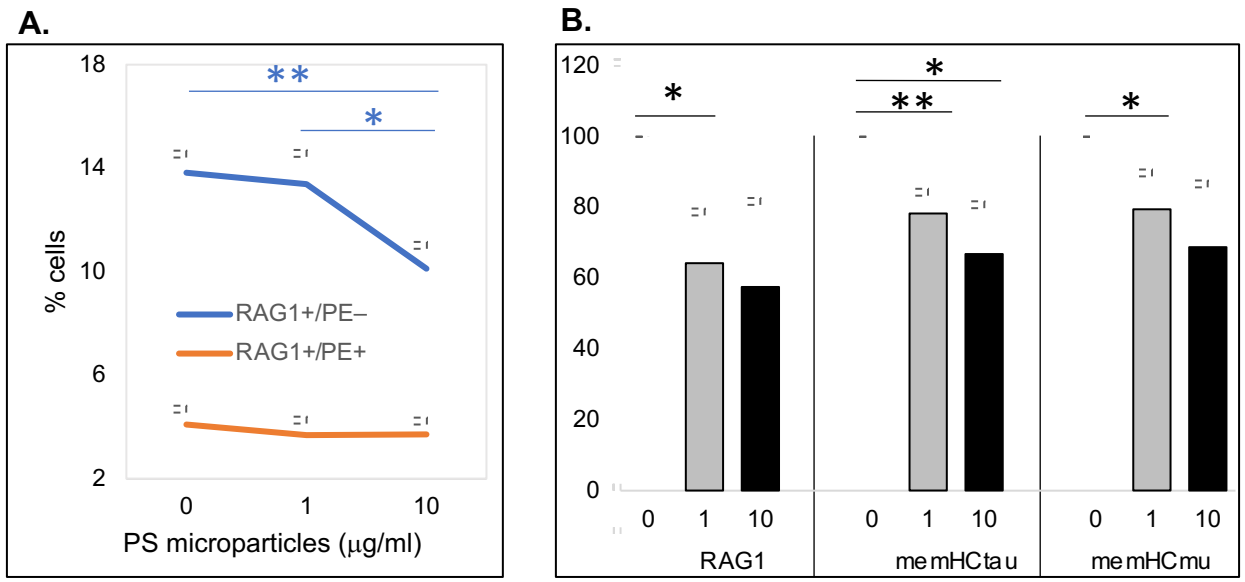
A.
B.
18
14
10
6
2
% cells
**
*
RAG1+/PE–
RAG1+/PE+
0
1
10
PS microparticles (μg/ml)
120
100
80
60
40
20
0
*
*
**
*
0
1
10
RAG1
memHCtau
memHCmu

Figure 6.

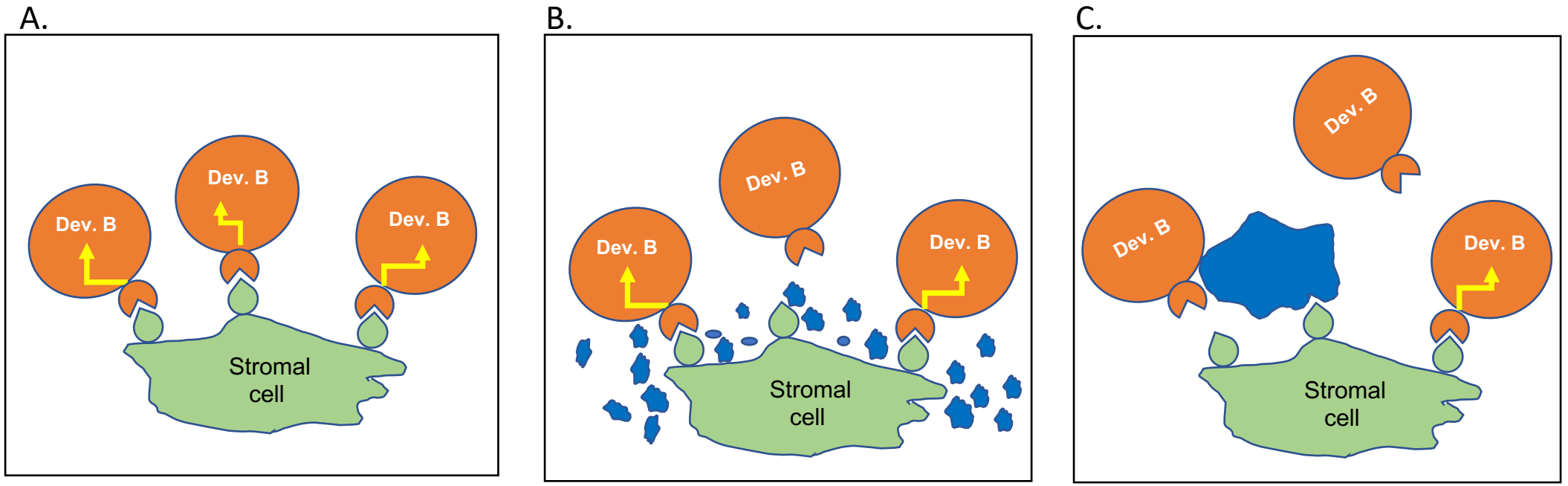
A.
Dev. B
Dev. B
Dev. B
Stromal cell
B.
Dev. B
Dev. B
Dev. B
Stromal cell
C.
Dev. B
Dev. B
Dev. B
Stromal cell

Figure 7.

Cell type	Pax5	HCmu	HCtau	Q4E	RAG1
Early developing B	+	low or –	–or low	+	+
(im)mature IgM+ B	+	+	–	–	–
(im)mature IgT+ B	+	–	+	–	–
Myeloid	–	–	–	+	–

Table I. Markers used to identify B and myeloid populations in the anterior kidney

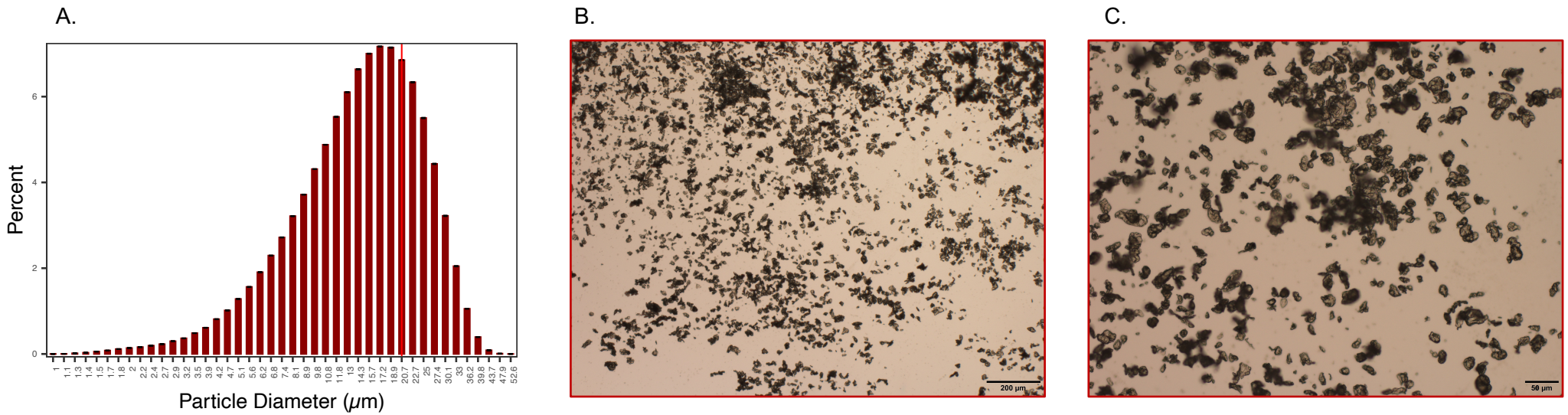

Supplemental Figure 1.

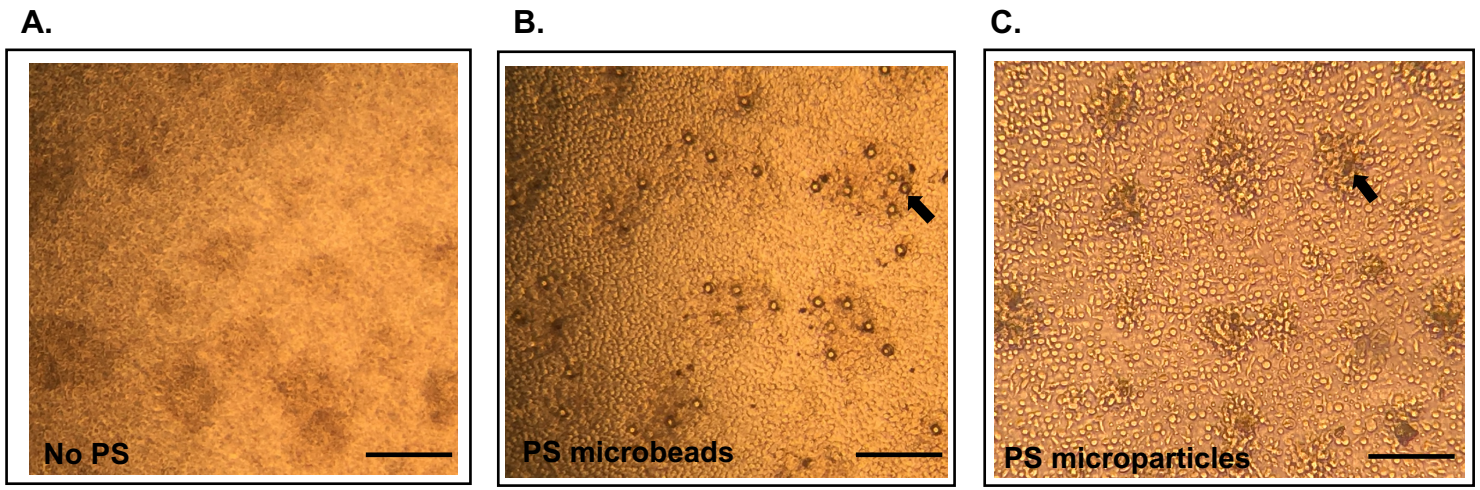

Supplemental Figure 2.